Removal of uranium(VI) from aqueous solution by *Camellia oleifera* shell-based activated carbon: adsorption equilibrium, kinetics, and thermodynamics

Zhengji Yi, Jian Liu, Rongying Zeng, Xing Liu, Jiumei Long and Binyan Huang

ABSTRACT

Camellia oleifera shell-based activated carbon (COSAC) was prepared by H_3PO_4 activation method and further used to remove U(VI) from the aqueous solution in a batch system. This research examined the influence of various factors affecting U(VI) removal, including contact time, pH, initial U(VI) concentration, and temperature. The results showed that the U(VI) adsorption capacity and removal efficiency reached 71.28 mg/g and 89.1% at the initial U(VI) concentration of 160 mg/L, temperature of 298 K, pH 5.5, contact time of 60 min, and COSAC dosage of 2.0 g/L. The pseudo-first-order, pseudo-second-order, and intraparticle diffusion equations were used to identify the optimum model that can describe the U(VI) adsorption kinetics. The pseudo-second-order kinetics model performed better in characterizing the adsorption system compared with the pseudo-first-order and intraparticle diffusion models. Isotherm data were also discussed with regard to the appropriacy of Langmuir, Freundlich, Temkin, and Dubinin–Radushkevich models. The Langmuir model described the U(VI) adsorption process the best with a maximum adsorption capacity of 78.93 mg/g. Thermodynamic analysis ($\Delta G^0 < 0$, $\Delta H^0 > 0$, and $\Delta S^0 > 0$) indicated that the U(VI) adsorption process is endothermic and spontaneous. All the results imply that COSAC has a promising application in the removal or recovery of U(VI) from aqueous solutions.

Key words | activated carbon, adsorption, *Camellia oleifera* shell, uranium

Zhengji Yi
Jian Liu (corresponding author)
Rongying Zeng
Xing Liu
Key Laboratory of Functional Metal-Organic Compounds of Hunan Province and Key Laboratory of Functional Organometallic Materials of College of Hunan Province, College of Chemistry and Material Science,
Heyang Normal University,
Hengyang 421008,
China
E-mail: *liujianzyx@126.com*

Jiumei Long
Binyan Huang
College of Life Sciences and Environment,
Hengyang Normal University,
Hengyang 421008,
China

HIGHLIGHTS

- Phosphoric acid activation method was used to prepare *Camellia oleifera* shell-based activated carbon (COSAC).
- COSAC features a high surface area and macroporous structure.
- The pH was one of the most critical parameters affecting the adsorption of U(VI).
- A good U(VI) adsorption performance was observed for COSAC.
- COSAC may be a promising adsorbent for uranium removal from wastewater.

INTRODUCTION

Along with the increase in anthropogenic production and living activities, various heavy metals and organic pollutants are discharged continuously into water bodies and soils each year (Djehaf *et al.* 2017; Igbanoi *et al.* 2019). For instance, leachates derived from municipal solid wastes often contain toxic chemicals and lead to the pollution of surface and groundwater (Iwuoha & Akinseye 2019). Notably, considerable attention is being paid to the pollution from heavy metals given that they are non-biodegradable, prone to accumulate in the environment, and likely to have deleterious effects on human beings and living organisms at low concentrations. In this respect, recent studies have focused

doi: 10.2166/wst.2020.504

on monitoring and evaluation of their potential ecotoxicity by means of bioassays using higher plants and natural bioluminescent bacteria as indicators (Iqbal 2016; Abbas *et al.* 2018; Iqbal *et al.* 2019). Dysfunction tests on the propagation of insects were applied to evaluate the degree of poisonous metal contamination in polluted areas (Sun *et al.* 2016). In summary, metal contamination poses a serious threat to human survival and has become one of the most pivotal environmental problems for global concern.

For instance, U(VI) is considered one of the typical heavy metal ions with chemical and radioactive toxicity. Because of its accumulation effect, the enrichment of U(VI) in biological tissues can result in severe diseases and damages to living organisms, including toxic hepatitis, skin corrosion, kidney damage, leukemia, genetic aberration, and cancer (Asic *et al.* 2017; Bjorklund *et al.* 2017). The World Health Organization has set the maximum allowable level of uranium in domestic water supplies at 15 μg/L (Banning & Benfer 2017). Given that the concentration of U(VI) is usually higher than the permissible levels, we must search for economic and effective methods for the removal and recycling of uranium from wastewater.

Various physicochemical methods have been developed to remove uranium from wastewater; these methods include solvent extraction, electrochemical treatment, oxidation–reduction method, reverse osmosis, ion exchange, chemical precipitation/flocculation, and membrane nano-filtration (Bhalara *et al.* 2014). However, these methods often have shortcomings, such as high operation cost, large energy consumption, incomplete metal removal, and generation of secondary contaminants. These shortcomings restrict the further application of these methods in large-scale in-situ operations. Adsorption stands out as one of the most effective methods in wastewater treatment and is commonly used in the removal of heavy metals worldwide (Abbas *et al.* 2017; Jennifer & Ifedi 2019; Alaqarbeh *et al.* 2020; Alkherraz *et al.* 2020; Awwad *et al.* 2020). Such wide usage of adsorption can be attributed to its advantages, such as easily obtainable sources, low operation cost, environmental friendliness, and minimization of sludge generation.

In recent years, the adsorption of U(VI) by metal oxides (Wang *et al.* 2013), layered double hydroxide composites using various intercalants (Zou *et al.* 2017; Chen *et al.* 2018; Reda *et al.* 2019), and amidoxime-based materials (Lu *et al.* 2017; Qin *et al.* 2017; Zeng *et al.* 2017), have been investigated. These materials exhibit relatively high uranium adsorption capacity. In addition, other investigators have demonstrated that a variety of agricultural and forestry wastes, such as citrus peel (Bhatti *et al.* 2016), *Musa paradisiaca* peels (Ibisi & Asoluka 2018), sweet potato peels (Chidi & Kelvin 2018), rice husk (Kausar *et al.* 2017), groundnut shell (Babarinde & Onyiaocha 2016), and modified *Vigna radiata* (Naeem *et al.* 2017) can be used as low-cost biosorbents to remove toxic heavy metal ions effectively.

Apart from the above agricultural and forestry residues, various carbonaceous materials were extensively used to remove radionuclides from aqueous solution. Sun *et al.* (2017) reported that the sorption of U(VI) by sulfonated graphene oxide was independent of ionic strength, and the maximum sorption capacity calculated from Langmuir model was 45.05 mg/g. Xu *et al.* (2020) investigated the adsorption of U(VI) by hyacinth-derived biochar and observed that the adsorption process can follow pseudo-second-order kinetics with a corresponding U(VI) adsorption capacity of 55.32 mg/g. Activated carbon is also one of the most important carbonaceous materials that can be widely applied in the biosorptive removal of heavy metals and other contaminants because it has a porous structure with a high surface area ranging from 600 m^2/g to 2,000 m^2/g (Lu *et al.* 2015; Legrouri *et al.* 2017). The removal of organomercurial compounds from wastewater by using activated carbons was examined and compared by using an ion exchange resin – Amberlite GT73 (Velicu *et al.* 2007). The adsorption capacity of activated carbons was greater than that of the ion exchange resin. Activated carbon-enhanced activated sludge process is also used to treat petroleum wastewater (Jafarinejad 2017). Many industrial, agricultural, and forestry residues, such as lignocellulosic waste (Seyyedeh et al. 2020), barley straw (Pallares *et al.* 2018), date press cake (Norouzi *et al.* 2018), walnut shell (Teixeira *et al.* 2019), guava seeds (Pezoti *et al.* 2016), loofah (Shih *et al.* 2020), and coal pitch (Zhong *et al.* 2016) can be used to prepare various activated carbons (Fazal-ur-Rehman 2018). Nonetheless, their adsorption performance toward various heavy metals is limited. Researchers should continue searching for cheap and easily available biomass that can be used to prepare activated carbon with high metal adsorption capacity.

Camellia oleifera is a woody oil-bearing tree species distributed specifically in South China, with the total cultivation area of up to 3.5×10^6 hm^2 and annual yield around 560 million tons (Fan *et al.* 2017). The seeds of *Camellia oleifera* are mainly used to produce high-grade tea oil, but most of *Camellia oleifera* shells are annually thrown away as agricultural wastes and used as fuels or fertilizers in the countryside. As one of the underused agricultural byproducts of *Camellia* oil, the shells are not only easily available but can also be converted into activated carbon

because they contain abundant lignin, hemicellulose, and cellulose. Furthermore, given that *Camellia oleifera* shells are inexpensive and nontoxic to the environment, we can turn such waste into a profitable material if the shells are processed into a high-performance adsorbent for use in the treatment of uranium-bearing wastewater. In this work, we used *Camellia oleifera* shells to prepare porous activated carbon with H_3PO_4 activation method. Afterward, the *Camellia oleifera* shell-based activated carbon (COSAC) was employed to remove U(VI) ions from an aqueous solution. The effects of various parameters affecting the removal of uranium ions by adsorption onto COSAC powder were investigated, and the results were analyzed in detail. The findings were followed up by the investigation of the proper isotherms and kinetics models. The present article aimed to evaluate the capability of COSAC to remove uranium ions from aqueous solutions.

MATERIALS AND METHODS

Chemical reagents

U_3O_8 was procured from the School of Nuclear Resources and Nuclear Fuel Engineering, University of South China. The other main chemicals, including Arsenazo III, H_3PO_4, HCl, H_2O_2, and HNO_3 were purchased from Sinopharm Chemical Reagent Company, Shanghai, China. All chemicals used in this research were of analytical pure grade.

Adsorbent preparation and characterization

Camellia oleifera shells were obtained from Xiayuan village, Xinxu town, Lanshan county, Hunan Province, Central China, during the picking season of *Camellia* fruit (Figure S1). The shells were rinsed with distilled water to eliminate the water-soluble impurities and dried in an oven at 105 °C for 6 h. The dried shells were crushed and milled to between 0.85 and 2.00 mm (10 and 20 mesh, respectively). Then, the milled *Camellia oleifera* shells were impregnated with concentrated phosphoric acid solution (shell:H_3PO_4 with 3:1 mass ratio) for 6 h and then dried at 105 °C for 24 h to remove water. Then, the dried samples were carbonized in a muffle furnace at 550 °C for 2 h to modify their porous structures. The resultant activated carbon was thoroughly rinsed with distilled water to remove the excess phosphorous compounds and then dried in a vacuum drying oven at 105 °C overnight. Finally, the activated carbon was cooled, crushed, and filtered. Only the activated carbon with the particle size distribution from 0.2 mm to 0.5 mm was collected and stored in a desiccator ready for use.

The quality test indexes of COSAC were determined in terms of the Chinese National Standard for Nut Shell Activated Carbon Test (No. GB/T 7702-1997). Scanning electron microscopy (SEM, Model S-4800 Hitachi, Tokyo, Japan) images were used to investigate the morphology and structure of the COSAC surface. The samples were fixed to a SEM stub using a conductive tape and sputter coated with gold.

Preparation of working solution

The stock solution of U(VI) (1,000 mg/L) was prepared by dissolving 1.1792 g U_3O_8 in a mixture of HCl, H_2O_2, and HNO_3 (Li *et al.* 2018). All working solutions were obtained by diluting the above stock solution with distilled water to achieve the desired concentrations. The initial pH was adjusted to the required values with dilute solutions of NaOH and HCl. The pH of the solutions was determined using a pHS-3C digital pH meter (Shanghai Leici Device Works, Shanghai, China) with a combined glass-calomel electrode.

Adsorption tests

The adsorption experiments were performed as a function of the initial pH, contact time, temperature, and initial U(VI) concentration in 250 mL conical flask containing 100 mL U(VI) solution in a thermostatic shaker. The initial solution pH (2.0–7.0), contact time (0–180 min), temperature (298–318 K), and initial U(VI) concentration (20–240 mg/L) were evaluated. Briefly, 0.2 g COSAC powder was added to a series of flasks, each containing 100 mL U(VI) solution. Then, the flasks were agitated on a reciprocal rotary shaker at 140 r/min. The solution was periodically monitored to analyze the concentration of U(VI) remaining in the solution using a standard Arsenazo-III method (Khan *et al.* 2006). All measurements were performed thrice, and average values were presented.

The U(VI) removal efficiency and adsorption capacity were calculated using the following equations to evaluate the U(VI) removal performance of COSAC powder (Ding *et al.* 2019):

$$R\ (\%) = \frac{(C_0 - C_t)}{C_0} \times 100 \quad (1)$$

$$q_t = \frac{(C_0 - C_t) \times V}{W} \quad (2)$$

$$q_e = \frac{(C_0 - C_e) \times V}{W} \quad (3)$$

where $R(\%)$ is the U(VI) removal efficiency; q_e and q_t are the U(VI) adsorption capacity (mg/g) at equilibrium and at any time t (min), respectively. C_0, C_t, and C_e are the initial U(VI) concentration, the remaining U(VI) concentration at any time t (min), and equilibrium U(VI) concentration (mg/L), respectively; V is the volume of aqueous solution (L); W is the weight of adsorbent used (g).

Kinetic investigations

Three kinetics models, namely, the pseudo-first-order, pseudo-second-order, and intraparticle diffusion models, were used to characterize the biosorption kinetics of U(VI) by COSAC. The integration form of the pseudo-first-order model is as follows (Lagergren 1898):

$$q_t = q_e(1 - e^{-k_1 t}) \tag{4}$$

where k_1 is the rate constant of the pseudo-first-order sorption (min^{-1}).

The pseudo-second-order model can be written as the following linear form (Blanchard *et al.* 1984):

$$\frac{t}{q_t} = \frac{t}{q_e} + \frac{1}{k_2 q_e^2} \tag{5}$$

where k_2 is the rate constant of pseudo-second-order adsorption [g/(mg·min)].

The intraparticle diffusion model can be written as the following linear form (Weber & Morris 1963):

$$q_e = k_{int} t^{1/2} + C \tag{6}$$

where k_{int} represents the intraparticle diffusion rate constant ($mg/(g \cdot min^{1/2})$), and C denotes the constant proportional to the extent of boundary layer thickness (mg/g).

Evaluation of equilibrium isotherms

The adsorption isotherms were evaluated by Langmuir, Freundlich, Temkin, and Dubinin–Radushkevich (D–R) models. Langmuir isotherm is based on the assumption that maximum adsorption occurs, a saturated monolayer of solute molecules exists on the adsorbent surface, and no interaction occurs between adsorbate molecules on the surface plane (Langmuir 1918). In other words, this model supposes a finite number of adsorption sites distributed homogeneously on the surface of the adsorbent (Equation (7)):

$$\frac{C_e}{q_e} = \frac{1}{q_{max}} C_e + \frac{1}{b q_{max}} \tag{7}$$

where q_{max} is the maximum amount of adsorption corresponding to the monolayer coverage (mg/g), and b is the Langmuir constant related to the adsorption energy (L/mg). The type of Langmuir isotherm can also be estimated based on whether the adsorption is favorable or unfavorable in terms of equilibrium parameter or dimensionless constant separation factor R_L, which can be defined as follows (Webi & Chakravort 1974):

$$R_L = \frac{1}{1 + b \times C_0} \tag{8}$$

where R_L indicates the adsorption process as irreversible ($R_L = 0$), favorable ($0 < R_L < 1$), linear ($R_L = 1$), or unfavorable ($R_L > 1$).

The Freundlich model, which depends on heterogeneous surfaces, proposes that adsorption sites are inequivalent and/or independent (Freundlich 1906). The linear Freundlich equation can be described as follows:

$$\ln q_e = \ln K_F + \frac{1}{n} \ln C_e \tag{9}$$

where K_F is the Freundlich constant indicating the adsorption capacity of the adsorbent ($mg^{(1-n)} \cdot g \cdot L^{-1}$), and n (dimensionless) is the Freundlich constant indicating adsorption intensity.

The Temkin model assumes that the adsorption heat decreases linearly with the surface coverage due to adsorbent–adsorbate interaction (Temkin 1941). The Temkin isotherm may be expressed as follows:

$$q_e = a \ln K_T + a \ln C_e \tag{10}$$

where K_T is an equilibrium parameter with regard to the maximum binding energy (L/g), and a is a dimensionless constant related to temperature and adsorption system.

The D–R isotherm assumes that the characteristics of the adsorption curves rely on the porosity of the adsorbent (Dubinin & Radushkevich 1947). The D–R isotherm

equation can be expressed as follows:

$$\ln q_e = \ln q_{DR} - \beta\varepsilon^2 \tag{11}$$

$$\varepsilon = RT\ln\left(1+\frac{1}{C_e}\right) \tag{12}$$

$$E = \frac{1}{\sqrt{2\beta}} \tag{13}$$

where q_{DR} is the theoretical monolayer adsorption capacity (mol/g), β (mol^2/J^2) is the D–R constant related to adsorption energy, ε (J^2/mol^2) is the Polanyi potential, and E is the mean adsorption energy that gives useful information about chemical and physical adsorption (kJ/mol).

Evaluation of adsorption thermodynamics

Thermodynamic parameters, including free energy change (ΔG^0), enthalpy change (ΔH^0), and entropy change (ΔS^0) related to the adsorption of U(VI) onto COSAC, can be calculated in terms of the following equations (Ho 2007):

$$\Delta G^0 = -RT\ln K_d \tag{14}$$

$$K_d = \frac{q_e}{C_e} \tag{15}$$

$$\ln K_d = \frac{\Delta S^0}{R} - \frac{\Delta H^0}{RT} \tag{16}$$

where R is the gas constant (8.314 J/(mol·K)), T is the absolute temperature (K), and K_d is the apparent equilibrium constant depending on temperature (mL/g).

RESULTS AND DISCUSSION

Characterization of COSAC

The quality testing indexes of COSAC were analyzed as follows: granularity diameter, 10 – 20 mesh; specific surface area, 1,300 m^2/g; total pore volume, 0.9 cm^3/g; pH, 8.4; ash content, ≤9%; strength, ≥91%; moisture content, ≤4%; iodine value, 960 mg/g; methylene blue value, 135 mg/g; residual chlorine adsorption rate, ≥85%. The surface morphology of raw COSAC before U(VI) adsorption and one reaction after U(VI) adsorption was observed by SEM (Figure 1). A rough, irregular, and porous texture appeared on the surface of raw COSAC. This surface assumed a fractured and fragmented pattern, which is a typical feature for carbonization of plant tissues (Figure 1(a) and 1(b)). Notably, this material had an unordered macroporous structure with pore diameters of 10–20 μm (pores with widths exceeding about 50 nm are called macropores). After U(VI) adsorption, an evident change in the surface morphology of COSAC was the disappearance of original macropores (Figure 1(c) and 1(d)). The U(VI) sequestration by numerous active groups on the COSAC surface might have caused the clogging of macropores. Moreover, COSAC featured a high Brunauer, Emmett, and Teller specific surface area of 1,300 m^2/g and a high total pore volume of 0.9 cm^3/g. In general, high surface area and appropriate porous structure are often pivotal features of high-performance adsorbents. Therefore, COSAC is likely to be a promising carbonaceous material for the adsorptive removal of U(VI) contaminant.

Effect of contact time and adsorption kinetics

Contact time is usually considered an important factor affecting the adsorption process. The adsorption of U(VI) proceeded relatively fast at the preliminary stage. Thus, the longer the adsorption process, the higher the U(VI) removal efficiency (Figure S2a). Then, the adsorption reached equilibrium at about 60 min, after which the U(VI) removal efficiency remained constant with the further increase in time. This phenomenon can be interpreted as follows. A high number of adsorption sites on the adsorbent surface were still empty at the initial stage. However, as the time elapsed, these empty sites were gradually occupied by adsorbate molecules, leading to the increase in U(VI) removal. When considerable active sites were occupied by adsorbate molecules, the adsorption experienced difficulty to proceed due to the repulsion between the solute molecules and the adsorbed layer. Hence, metal adsorption at the late stage was relatively slow before reaching equilibrium. Fasfous & Dawoud (2012) investigated the binding of U(VI) by multi-walled carbon nanotubes and confirmed that the time required to reach equilibrium was also approximately 60 min. By contrast, Caccin *et al.* (2013) reported a longer equilibrium time of about 48 h for the uptake of U(VI) on activated carbon derived from coconut shells.

The kinetics parameters in Equations (4)–(6) can be obtained from the curve fittings in Figure S2(b)–S2(d), and the fitted results are listed in Table 1. The R^2 values of pseudo-first-order and intraparticle diffusion models were distant from 1.0. Thus, neither of the two models can appropriately describe the U(VI) adsorption kinetics due to the evident void of linear correlation. However, the situation

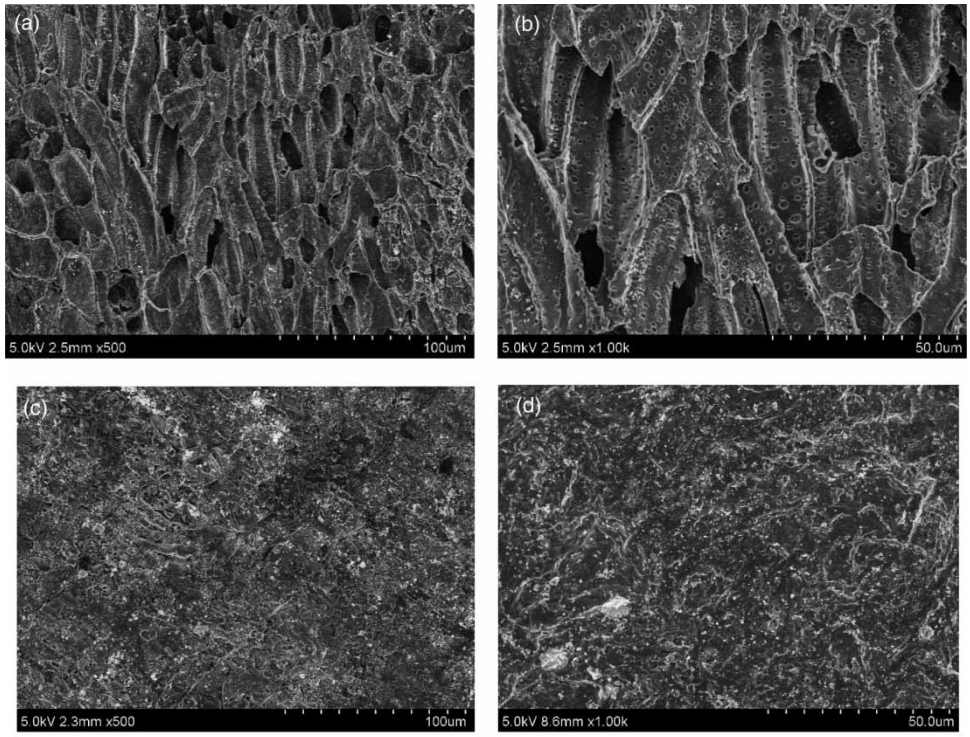

Figure 1 | SEM micrographs of COSAC at various magnifications (a and b: before uranium adsorption; c and d: after uranium adsorption).

Table 1 | Kinetics parameters for U(VI) adsorption onto COSAC

Model	Parameter	Value
Pseudo-first-order	k_1 (min^{-1})	0.061
	q_e (mg/g)	71.11
	R^2	0.9339
Pseudo-second-order	k_2 (g/(mg·min))	0.003
	q_e (mg/g)	72.46
	R^2	0.9946
	q_{exp} (mg/g)	71.81
Intraparticle diffusion	K_{int}	6.228
	C	21.89
	R^2	0.9367

differed for pseudo-second-order model. Not only the R^2 value of the model (0.9946) was very close to 1.0, but the theoretical value of q_e calculated from the model (72.46 mg/g) was close to the observed experimental value ($q_{exp} = 71.81$ mg/g). Therefore, the adsorption of U(VI) onto COSAC follows the pseudo-second-order model considerably better than the other two models. Thus, pseudo-second-order model can be appropriately used to describe the adsorption kinetics. Although our result is similar to that of previous research on the U(VI) adsorption by olive stone-based activated carbon and magnetic Fe/Zn layered double oxide@carbon nanotube, which also followed pseudo-second-order kinetics (Kutahyali & Eral 2010; Chen *et al.* 2018), it differed from that of an earlier report on the U(VI) adsorption by activated carbon from coconut shell, which followed pseudo-first-order kinetics (Caccin *et al.* 2013).

The pseudo-second-order kinetics model is based on the assumption that the rate-limiting step may be chemical adsorption. Based on the above analysis, chemical adsorption is the dominant mechanism for U(VI) removal by COSAC. The key factor determining the adsorption rate is the chemical reactions occurring between the active sites on the COSAC surface and U(VI) in solution.

Effect of pH

Wastewater treatment using traditional or untraditional adsorbents is highly dependent on the acidity or alkalinity of effluent because it influences the aquatic chemistry of heavy metals and the surface charge of adsorbents. The adsorption of U(VI) onto COSAC was carried out over the wide pH range from 2.0 to 7.0 (Figure 2). R and q increased

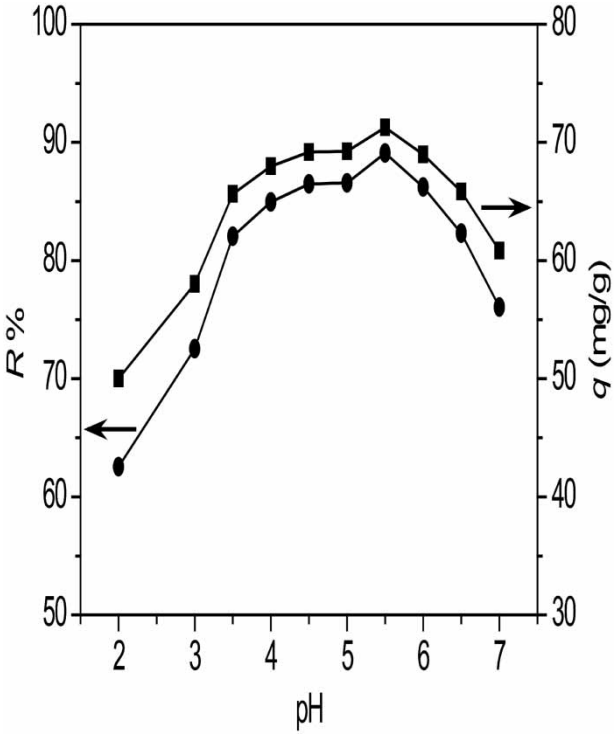

Figure 2 | Effect of pH on U(VI) adsorption by COSAC (temperature: 298 K; contact time: 60 min; COSAC dosage: 2.0 g/L (w/v); U(VI) concentration: 160 mg/L; solution volume: 100 mL).

with the increase in pH until the maximum value at pH 5.5, at which the maximum R and q were 89.1% and 71.28 mg/g, respectively, was reached. Afterward, the values decreased when the pH value exceeded 5.5. These results can be interpreted as follows. The activated carbon surface was coated with numerous active functional groups (hydroxyl, carboxyl, phosphate, etc.) with electrostatic adsorption capability. The solution pH was relatively low, uranium existed as the uncoordinated form of uranyl (UO_2^{2+}) ions in the aqueous solution, and the aforementioned functional groups on the surface of COSAC were protonized and positively charged. Thus, COSAC displayed a weak U(VI) adsorption performance owing to the strong repelling force between uranyl ions and protonized functional groups. Accompanied with the increase in pH, these functional groups on the COSAC surface were progressively deprotonized and negatively charged. The electrostatic affinity between the functional groups with negative charges and uranyl was augmented, thus leading to increased U(VI) removal. As the solution pH was further increased beyond 5.5, U(VI) was prone to exist as stable forms of uranyl-carbonato and uranyl-hydroxyl-carbonato complexes, e.g. $[UO_2(CO_3)_2]^{2-}$, $[UO_2(CO_3)_3]^{4-}$, and $[(UO_2)_2(CO_3)(OH)_3]^{-}$, in the solution (Fox *et al.* 2019). The shift in uranium speciation can hinder its adsorption process because of the electrostatic repulsion between the negatively-charged uranyl complexes and functional groups with negative charges. In addition, the volume of uranyl complex molecules is extremely large, which may be unbeneficial to their adsorption. Our results differ from those of previous research on the adsorption of U(VI) by graphene oxide-supported uniform magnetite nanoparticle composites, in which the U(VI) removal reached the maximum at the neutral pH range (6.0–8.0) and dropped slightly beyond pH 8.0 (Ding *et al.* 2017). According to the above analysis, a pH 5.5 was selected as the equilibrium time for other experiments.

Effect of initial U(VI) concentration and adsorption isotherm study

Adsorption isotherm can be used to delineate the relationship between the amount of a solute adsorbed and its concentration in the equilibrium solution at a fixed temperature. In addition, studies should focus on gaining insights into the adsorbent–adsorbate interactions, estimate the adsorption capacity of adsorbents, and optimize adsorbent applications. In this work, adsorption experiments were carried out at the initial U(VI) concentration range of 40 mg/L to 240 mg/L. Evidently, the U(VI) adsorption equilibrium capacity increased with increase in the concentration of U(VI) (Figure 3). The equilibrium data for the U(VI) – COSAC adsorption system were further fitted using the Langmuir, Freundlich, D-R, and Temkin isotherms (Figure S3). Table 2 presents the corresponding parameters and R^2 values for the four isotherm models. The R^2 values of Freundlich, D-R, and Temkin isotherms were far from 1.0, suggesting that the adsorption onto COSAC cannot be described by these three isotherms. By contrast, the R^2 value of Langmuir isotherm was notably closer to 1.0. Hence, the adsorption of U(VI) onto COSAC can be best characterized by the Langmuir model, and the monolayer maximum capacity was 78.93 mg/g. Additionally, the R_L values obtained were in the range of 0–1 for U(VI) concentrations of 40 mg/L–240 mg/L (Table 2), indicating the favorable adsorption of U(VI) onto COSAC.

q_{max} is an important index for characterizing the adsorption performance of adsorbents and considered a pivotal parameter for engineering design. Previous studies have reported the q_{max} values of other carbonaceous materials for U(VI) adsorption, e.g. 20.76 mg/g for montmorillonite@-carbon composite (Zhang *et al.* 2015), 39.1 mg/g for multiwalled carbon nanotubes (Fasfous & Dawoud 2012),

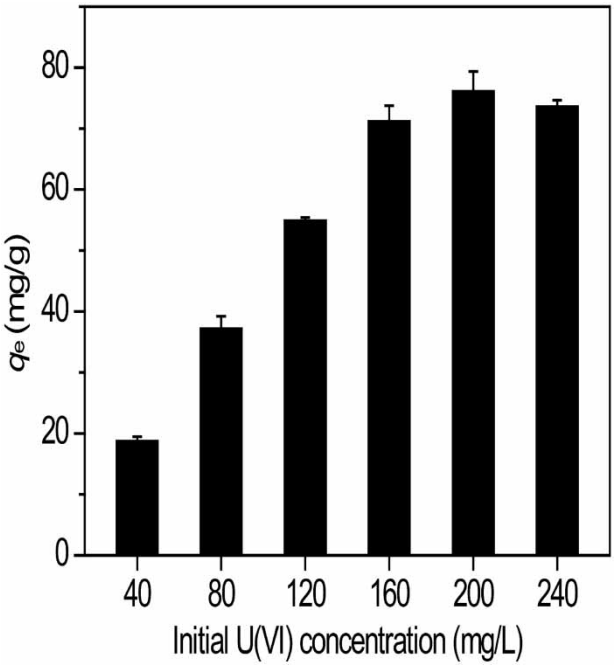

Figure 3 | Effect of initial U(VI) concentration on its adsorption by COSAC (temperature: 298 K; pH: 5.5; contact time: 60 min; COSAC dosage: 2.0 g/L (w/v); solution volume: 100 mL).

Table 2 | Isotherm parameters for U(VI) adsorption by COSAC

Model	Parameter	Value
Langmuir	q_{max} (mg/g)	78.93
	b (L/mg)	0.2146
	R^2	0.9941
	R_L	0.0191–0.1043
Freundlich	K_F ($mg^{(1-n)}\cdot g\cdot L^{-1}$)	16.66
	n	2.814
	R^2	0.7362
D–R	q_{DR} (mg/g)	303.8
	β (mol^2/J^2)	3.076×10^{-9}
	E_{DR} (kJ/mol)	12.71
	R^2	0.7916
Temkin	K_T	2.352
	a	15.66
	R^2	0.8207

46.2 mg/g for Arsenazo-functionalized magnetic carbon composite (Li *et al.* 2018), 67.9 mg/g for amidoxime-modified multiwalled carbon nanotubes (Wu *et al.* 2018), and 163 mg/g for carbonaceous spheres from glucose (Cai *et al.* 2016). The q_{max} of COSAC (78.93 mg/g) in our work is notably greater than most of the above-mentioned carbonaceous materials. Thus, COSAC may be regarded as a potential high-performance adsorbent for U(VI) removal.

Table 3 | Thermodynamic parameters of uranium binding by COSAC

ΔH^0 (kJ/mol)	ΔS^0 (J/(mol·K))	ΔG^0 (kJ/mol)		
		298 K	308 K	318 K
17.37	70.06	−3.488	−4.245	−4.887

Adsorption thermodynamics study

To evaluate the effect of temperature on the U(VI) adsorption by COSAC, the U(VI) removal capability was examined at different temperatures (298, 308, and 318 K). U(VI) adsorption decreased from 71.28 mg/g to 74.16 mg/g with the increase in temperature from 298 to 318 K (Figure S4). The thermodynamic parameters (ΔG^0, ΔH^0, and ΔS^0) were calculated (Table 3). The negative value of ΔG^0 indicates the spontaneous nature of adsorption of U(VI) by COSAC for all the tested temperatures. The ΔG^0 value became more negative with the increase in temperature, indicating that the adsorption process was favorable at high temperatures. The positive value of ΔH^0 confirmed the endothermic nature of removal process, whereas the positive value of ΔS^0 suggests that this adsorption will result in increased randomness. Similar results have been reported for U(VI) adsorption onto other carbonaceous adsorbents (Zhou *et al.* 2015; Sun *et al.* 2017). In short, the adsorption of U(VI) by COSAC may be an enthalpically unfavorable (endothermic) and entropy-driven spontaneous process in nature.

CONCLUSION

In this work, characterization, uranium adsorption tests, adsorption equilibrium, and kinetics studies of COSAC were conducted to examine its U(VI) adsorption capability and to understand the corresponding adsorption mechanism. The adsorption of U(VI) on COSAC was investigated as a function of contact time, solution pH, and adsorbate concentration. The contact time of 60 min was sufficient to attain equilibrium. Kinetics data fit very well the pseudo-second-order model, suggesting that chemical adsorption is the rate-limiting step. The optimum pH for the maximum removal of U(VI) was observed at pH 5.5. The isotherm adsorption data were modeled best by the linear Langmuir equation with the monolayer adsorption capacity of

78.93 mg/g, which was comparable to those reported in literature. Thermodynamic calculations suggest that the adsorption process was endothermic, spontaneous, and accompanied by the increase in entropy. Overall, COSAC can be a highly attractive candidate for the effective removal of uranium from wastewater. Regeneration of the adsorbent and column experiments were subject to further research.

ACKNOWLEDGEMENTS

This research was sponsored by National Natural Science Foundation of China (No. 41773133), the Science and Technology Development Project of Hengyang City (No. 2019yj011171), and the Center for the Functionalization of Metal-Organic Frameworks Materials Studies.

DATA AVAILABILITY STATEMENT

All relevant data are included in the paper or its Supplementary Information.

REFERENCES

Abbas, G., Javed, I., Iqbal, M., Haider, R., Hussain, F. & Qureshi, N. 2017 Adsorption of non-steroidal anti-inflammatory drugs (diclofenac and ibuprofen) from aqueous medium onto activated onion skin. *Desalination & Water Treatment* **95**, 274–285.

Abbas, M., Adil, M., Ehtisham-ul-Haque, S., Munir, B., Yameen, M., Ghaffar, A., Shar, G. A., Asif Tahir, M. & Iqbal, M. 2018 *Vibrio fischeri* bioluminescence inhibition assay for ecotoxicity assessment: a review. *Science of The Total Environment* **626**, 1295–1309.

Alaqarbeh, M., Shammout, M. & Awwad, A. 2020 Nano platelets kaolinite for the adsorption of toxic metal ions in the environment. *Chemistry International* **6** (2), 49–55.

Alkherraz, A. M., Ali, A. K. & Elsherif, K. M. 2020 Removal of Pb(II), Zn(II), Cu(II) and Cd(II) from aqueous solutions by adsorption onto olive branches activated carbon: equilibrium and thermodynamic studies. *Chemistry International* **6** (1), 11–20.

Asic, A., Kurtovic-Kozaric, A., Besic, L., Mehinovic, L., Hasic, A., Kozaric, M., Hukic, M. & Marjanovic, D. 2017 Chemical toxicity and radioactivity of depleted uranium: the evidence from in vivo and in vitro studies. *Environmental Research* **156**, 665–673.

Awwad, A. M., Amer, M. W. & Al-Aqarbeh, M. M. 2020 TiO_2-kaolinite nanocomposite prepared from the Jordanian kaolin clay: adsorption and thermodynamic of Pb(II) and Cd(II) ions in aqueous solution. *Chemistry International* **6** (4), 168–178.

Babarinde, A. & Onyiaocha, G. O. 2016 Equilibrium sorption of divalent metal ions onto groundnut (*Arachis hypogaea*) shell: kinetics, isotherm and thermodynamics. *Chemistry International* **2** (1), 37–46.

Banning, A. & Benfer, M. 2017 Drinking water uranium and potential health effects in the German Federal State of Bavaria. *International Journal of Environmental Research and Public Health* **14** (8), 927.

Bhalara, P. D., Punetha, D. & Balasubramanian, K. 2014 A review of potential remediation techniques for uranium(VI) ion retrieval from contaminated aqueous environment. *Journal of Environmental Chemical Engineering* **2** (3), 1621–1634.

Bhatti, H. N., Zaman, Q., Kausar, A., Noreen, S. & Iqbal, M. 2016 Efficient remediation of Zr(IV) using citrus peel waste biomass: kinetic, equilibrium and thermodynamic studies. *Ecological Engineering* **95**, 216–228.

Bjorklund, G., Christophersen, O. A., Chirumbolo, S., Selinus, O. & Aaseth, J. 2017 Recent aspects of uranium toxicology in medical geology. *Environmental Research* **156**, 526–533.

Blanchard, G., Maunaye, M. & Martin, G. 1984 Removal of heavy metals from waters by means of natural zeolites. *Water Research* **18** (12), 1501–1507.

Caccin, M., Giacobbo, F., Da Ros, M., Besozzi, L. & Mariani, M. 2013 Adsorption of uranium, cesium and strontium onto coconut shell activated carbon. *Journal of Radioanalytical and Nuclear Chemistry* **297** (1), 9–18.

Cai, H. M., Lin, X. Y., Tian, L. Y. & Luo, X. G. 2016 One-step hydrothermal synthesis of carbonaceous spheres from glucose with an aluminum chloride catalyst and its adsorption characteristic for uranium(VI). *Industrial & Engineering Chemistry Research* **55** (36), 9648–9656.

Chen, H., Zhang, Z., Wang, X., Chen, J., Xu, C., Liu, Y., Yu, Z. & Wang, X. 2018 Fabrication of magnetic Fe/Zn layered double oxide@carbon nanotube composites and their application for U(VI) and ^{241}Am(III) removal. *ACS Applied Nano Materials* **1**, 2386–2396.

Chidi, O. & Kelvin, R. 2018 Surface interaction of sweet potato peels (*Ipomoea batata*) with Cd(II) and Pb(II) ions in aqueous medium. *Chemistry International* **4** (1), 221–229.

Ding, C., Cheng, W., Nie, X. & Yi, F. 2017 Synergistic mechanism of U(VI) sequestration by magnetite-graphene oxide composites: evidence from spectroscopic and theoretical calculation. *Chemical Engineering Journal* **324**, 113–121.

Ding, H. L., Zhang, X. N., Yang, H., Zhang, Y. & Luo, X. G. 2019 Biosorption of U(VI) by active and inactive *Aspergillus niger*: equilibrium, kinetic, thermodynamic and mechanistic analyses. *Journal of Radioanalytical and Nuclear Chemistry* **319** (3), 1261–1275.

Djehaf, K., Bouyakoub, A. Z., Ouhib, R., Benmansour, H., Bentouaf, A., Mahdad, A., Moulay, N., Bensaid, D. & Ameri, M. 2017 Textile wastewater in Tlemcen (Western Algeria): impact, treatment by combined process. *Chemistry International* **3** (4), 414–419.

Dubinin, M. M. & Radushkevich, L. V. 1947 Equation of the characteristic curve of activated charcoal. *Proceedings of the*

Union of Soviet Socialist Republics Academy of Sciences **79** (7), 843–848.

Fan, F. Y., Zheng, Y. W., Huang, Y. B., Lu, Y., Wang, Z., Chen, B. & Zheng, Z. F. 2017 Preparation and characterization of biochars from waste *Camellia oleifera* shells by different thermochemical processes. *Energy & Fuels* **31** (8), 8146–8151.

Fasfous, I. I. & Dawoud, J. N. 2012 Uranium(VI) sorption by multiwalled carbon nanotubes from aqueous solution. *Applied Surface Science* **259**, 433–440.

Fazal-ur-Rehman, M. 2018 Current scenario and future prospects of activated carbon preparation from agro-industrial wastes: a review. *Chemistry International* **4** (2), 109–119.

Fox, P. M., Tinnacher, R. M., Cheshire, M. C., Caporuscio, F., Carrero, S. & Nico, P. S. 2019 Effects of bentonite heating on U(VI) adsorption. *Applied Geochemistry* **109**, 104392.

Freundlich, H. M. F. 1906 Over the adsorption in solution. *Journal of Physical Chemistry A* **57**, 385–470.

Ho, Y. S. 2007 Removal of copper ions from aqueous solution by tree fern. *Water Research* **37** (10), 2323–2330.

Ibisi, N. E. & Asoluka, C. A. 2018 Use of agro-waste (*Musa paradisiaca* peels) as a sustainable biosorbent for toxic metal ions removal from contaminated water. *Chemistry International* **4** (1), 52–59.

Igbanoi, F. J., Ihunda, I. E. & Iwuoha, G. N. 2019 Leachates and physicochemical characteristics of Rumuodumaya dumpsites, Niger-Delta, Nigeria. *Chemistry International* **5** (2), 126–131.

Iqbal, M. 2016 *Vicia faba* bioassay for environmental toxicity monitoring: a review. *Chemosphere* **144**, 785–802.

Iqbal, M., Abbas, M., Nazir, A. & Qamar, A. Z. 2019 Bioassays based on higher plants as excellent dosimeters for monitoring: a review. *Chemistry International* **5** (1), 1–80.

Iwuoha, G. N. & Akinseye, A. 2019 Toxicological symptoms and leachates quality in Elelenwo, Rivers State. *Nigeria. Chemistry International* **5** (3), 198–205.

Jafarinejad, S. 2017 Activated sludge combined with powdered activated carbon (PACT process) for the petroleum industry wastewater treatment: a review. *Chemistry International* **3** (4), 368–377.

Jennifer, E. C. & Ifedi, O. P. 2019 Modification of natural bentonite clay using cetyl trimetyl-ammonium bromide and its adsorption capability on some petrochemical wastes. *Chemistry International* **5** (4), 269–273.

Kausar, A., Bhatti, H. N., Iqbal, M. & Ashraf, A. 2017 Batch versus column modes for the adsorption of radioactive metal onto rice husk waste: conditions optimization through response surface methodology. *Water Science and Technology* **76** (5), 1035–1043.

Khan, M. H., Warwick, P. & Evans, N. 2006 Spectrophotometric determination of uranium with arsenazo III in perchloric acid. *Chemosphere* **63** (7), 1165–1169.

Kutahyali, C. & Eral, M. 2010 Sorption studies of uranium and thorium on activated carbon prepared from olive stones: kinetic and thermodynamic aspects. *Journal of Nuclear Materials* **396** (2–3), 251–256.

Lagergren, S. 1898 About the theory of so-called adsorption of soluble substances. *Kungliga Svenska Vetenskapsakademiens Handlingar* **24** (4), 1–39.

Langmuir, I. 1918 The adsorption of gases on plane surface of glass, mica and platinum. *Journal of the American Chemical Society* **40** (9), 1361–1403.

Legrouri, K., Khouya, E., Hannache, H., El Hartti, M., Ezzine, M. & Naslain, R. 2017 Activated carbon from molasses efficiency for Cr(VI), Pb(II) and Cu(II) adsorption: a mechanistic study. *Chemistry International* **3** (3), 301–310.

Li, P., Wang, J. J., Wang, X. L., He, B. H., Pan, D. Q., Liang, J. J., Wang, F. K. & Fan, Q. H. 2018 Arsenazo functionalized magnetic carbon composite for uranium(VI) removal from aqueous solution. *Journal of Molecular Liquids* **269**, 441–449.

Lu, L. X., Zhao, H. B., Lu, Y., Wang, G. W., Mao, Y. L., Wang, X., Liu, K., Liu, X. F., Zhao, Q. & Jiang, T. S. 2015 Removal characteristics of Cd(II) ions from aqueous solution on ordered mesoporous carbon. *Korean Journal of Chemical Engineering* **32** (10), 2161–2167.

Lu, X., Zhang, D., Tesfay Reda, A., Liu, C., Yang, Z., Guo, S., Xiao, S. & Ouyang, Y. 2017 Synthesis of amidoxime-grafted activated carbon fibers for efficient recovery of uranium(VI) from aqueous solution. *Industrial & Engineering Chemistry Research* **56** (41), 11936–11947.

Naeem, H., Bhatti, H. N., Sadaf, S. & Iqbal, M. 2017 Uranium remediation using modified *Vigna radiata* waste biomass. *Applied Radiation and Isotopes* **123**, 94–101.

Norouzi, S., Heidari, M., Alipour, V., Rahmanian, O. & Dindarloo, K. 2018 Preparation, characterization and Cr(VI) adsorption evaluation of NaOH-activated carbon produced from Date Press Cake; an agro-industrial waste. *Bioresource Technology* **258**, 48–56.

Pallares, J., Gonzalez-Cencerrado, A. & Arauzo, I. 2018 Production and characterization of activated carbon from barley straw by physical activation with carbon dioxide and steam. *Biomass and Bioenergy* **115**, 64–73.

Pezoti, O., Cazetta, A. L., Bedin, K. C., Souza, L. S. & Almeida, V. C. 2016 NaOH activated carbon of high surface area produced from guava seeds as a high-efficiency adsorbent for amoxicillin removal: kinetic, isotherm and thermodynamic studies. *Chemical Engineering Journal* **288**, 778–788.

Qin, Z., Ren, Y., Shi, S., Yang, C., Yu, J., Wang, S., Jia, J., Yu, H. & Wang, X. 2017 The enhanced uranyl-amidoxime binding by the electron-donating substituents. *RSC Advances* **7** (30), 18639–18642.

Reda, A. T., Zhang, D. & Lu, X. 2019 Intercalation of glycine into hydroxy double salt and its adsorption performance towards uranium(VI). *Environmental Technology & Innovation* **16**, 100474.

Seyyedeh, M. K., Nourollah, M., Mohammad, M. D. & Mohsen, S. 2020 A novel post-modification of powdered activated carbon prepared from lignocellulosic waste through thermal tension treatment to enhance the porosity and heavy metals adsorption. *Powder Technology* **366**, 358–368.

Shih, Y. J., Dong, C. D., Huang, Y. H. & Huang, C. P. 2020 Loofah derived activated carbon supported on nickel foam (AC/Ni) electrodes for the electro-sorption of ammonium ion from aqueous solutions. *Chemosphere* **242**, 125259.

Sun, H., Wu, W., Guo, J., Xiao, R., Jiang, F., Zheng, L. & Zhang, G. 2016 Effects of nickel exposure on testicular function, oxidative stress, and male reproductive dysfunction in *Spodoptera litura* Fabricus. *Chemosphere* **148**, 178–187.

Sun, Y., Wang, X., Ai, Y., Yu, Z., Huang, W., Chen, C., Hayat, T., Alsaedi, A. & Wang, X. 2017 Interaction of sulfonated graphene oxide with U(VI) studied by spectroscopic analysis and theoretical calculations. *Chemical Engineering Journal* **310**, 292–299.

Teixeira, S., Delerue-Matos, C. & Santos, L. 2019 Application of experimental design methodology to optimize antibiotics removal by walnut shell based activated carbon. *Science of The Total Environment* **646**, 168–176.

Temkin, M. I. 1941 Adsorption equilibrium and the kinetics of processes on nonhomogeneous surfaces and in the interaction between adsorbed molecules. *Zhurnal Fizicheskoi Khimii* **15**, 296–332.

Velicu, M., Fu, H., Suri, R. P. & Woods, K. 2007 Use of adsorption process to remove organic mercury thimerosal from industrial process wastewater. *Journal of Hazardous Materials* **148** (3), 599–605.

Wang, Z., Lee, S., Catalano, G., Lezama-pacheco, J. S., Bargar, J. R., Tebo, B. M. & Giammar, D. E. 2013 Adsorption of uranium(VI) to manganese oxides: X-ray absorption spectroscopy and surface complexation modeling. *Environmental Science and Technology* **47** (2), 850–858.

Weber, W. J. & Morris, J. C. 1963 Kinetics of adsorption on carbon from solutions. *Journal of the Sanitary Engineering Division by American Society of Civil Engineers* **89** (2), 31–63.

Webi, T. W. & Chakravort, R. K. 1974 Pore and solid diffusion models for fixed bed adsorbents. *AIChE Journal* **20** (2), 228–238.

Wu, J. L., Tian, K. & Wang, J. L. 2018 Adsorption of uranium (VI) by amidoxime modified multiwalled carbon nanotubes. *Progress in Nuclear Energy* **106**, 79–86.

Xu, Z., Xing, Y., Ren, A., Ma, D. & Hu, S. 2020 Study on adsorption properties of water hyacinth-derived biochar for uranium(VI). *Journal of Radioanalytical and Nuclear Chemistry* **324** (3), 1317–1327.

Zeng, J., Zhang, H., Sui, Y., Hu, N., Ding, D., Wang, F., Xue, J. & Wang, Y. 2017 New amidoxime-based material TMP-g-AO for uranium adsorption under seawater conditions. *Industrial & Engineering Chemistry Research* **56** (17), 5021–5032.

Zhang, R., Chen, C. L., Li, J. & Wang, X. K. 2015 Preparation of montmorillonite@carbon composite and its application for U(VI) removal from aqueous solution. *Applied Surface Science* **349** (15), 129–137.

Zhong, L. C., Zhang, Y. S., Ji, Y., Norris, P. & Pan, W. P. 2016 Synthesis of activated carbon from coal pitch for mercury removal in coal-fired power plants. *Journal of Thermal Analysis and Calorimetry* **123**, 851–860.

Zhou, L. M., Huang, Z. W., Luo, T. A., Jia, Y. Y., Liu, Z. R. & Adesina, A. A. 2015 Biosorption of uranium(VI) from aqueous solution using phosphate-modified pine wood sawdust. *Journal of Radioanalytical and Nuclear Chemistry* **303** (3), 1917–1925.

Zou, Y., Liu, Y., Wang, X., Sheng, G., Wang, S., Ai, Y., Ji, Y., Liu, Y., Hayat, T. & Wang, X. 2017 Glycerol-modified binary layered double hydroxide nanocomposites for uranium immobilization via extended X-ray absorption fine structure technique and density functional theory calculation. *ACS Sustainable Chemistry & Engineering* **5** (4), 3583–3595.

First received 21 June 2020; accepted in revised form 8 October 2020. Available online 21 October 2020